

AperTO - Archivio Istituzionale Open Access dell'Università di Torino

Fast carbon dioxide recycling by reaction with γ -Mg(BH₄)₂

This is the author's manuscript

Original Citation:

Availability:

This version is available <http://hdl.handle.net/2318/151491> since 2016-01-06T10:24:58Z

Published version:

DOI:10.1039/C4CP03300K

Terms of use:

Open Access

Anyone can freely access the full text of works made available as "Open Access". Works made available under a Creative Commons license can be used according to the terms and conditions of said license. Use of all other works requires consent of the right holder (author or publisher) if not exempted from copyright protection by the applicable law.

(Article begins on next page)



UNIVERSITÀ DEGLI STUDI DI TORINO

This is an author version of the contribution published on:

Questa è la versione dell'autore dell'opera:

Fast carbon dioxide recycling by reaction with γ -Mg(BH₄)₂

Jenny G. Vitillo, Elena Groppo, Elisa Gil Bardají, Marcello Baricco, Silvia Bordigaa,

Phys. Chem. Chem. Phys., 2014,16, 22482-22486

DOI: 10.1039/C4CP03300K

The definitive version is available at:

La versione definitiva è disponibile alla URL:

<http://pubs.rsc.org/en/Content/ArticleLanding/2014/CP/C4CP03300K#!divAbstract>

Fast carbon dioxide recycling by reaction with γ -Mg(BH₄)₂

Jenny G. Vitillo,^{*a,b} Elena Groppo,^a Elisa Gil Bardají,^c Marcello Baricco,^a Silvia Bordiga^a

γ -Mg(BH₄)₂ was found to be a promising material for CO₂ recycling (mainly to formate and alkoxide-like compounds). CO₂ conversion occurs with unprecedented fast kinetics at 30°C and 1 bar. A multi-technique approach allowed to ascribe superior performances to its large specific surface area.

Porous complex hydrides are a new class of materials in the panorama of metal hydrides.¹ Among them, gamma phase of Mg(BH₄)₂ possesses the interesting peculiarity to show a large permanent porosity, accounting for about the 33% of the material volume (see Fig. 1).¹ Its structure is constituted by Mg²⁺ ions in tetrahedral coordination, linked through a shared [BH₄]⁻, giving rise to an highly 3D porous structure characterized by hexagonal overtures with a narrowest dimension of 5.95 Å (geometrical distance). Each hexagon, having a chair conformation, shares every Mg-BH₄-Mg side with a vicinal hexagon through a tetrahedral angle. The high surface of this material (1160 m² g⁻¹) makes it interesting as nanosponge for gas adsorption and its ability to adsorb large quantities of molecular hydrogen was recently reported.¹

Carbon dioxide is generally recognized as the most important greenhouse gas. The astonishing increase in CO₂ concentration in the terrestrial atmosphere in the past 200 years (from 270 to 399 ppmv, amounting to approximately 900 Gt CO₂)²⁻⁴ and, moreover, its monotonic trend are expected to have important fallout on the climate of the planet. In fact, a linear dependence of the terrestrial temperature on the CO₂ concentration has been experimentally determined,² estimating an increase of 13.5°C per 130 ppmv of CO₂, with important consequences for example on the sea level.⁵ It is then evident the necessity to employ selective sorbers that capture CO₂ in order to reduce the anthropogenic emissions, either by molecular adsorption or by dissociative chemisorptions. Among the first class of materials, it was demonstrated that magnesium cations have a larger affinity toward CO₂ with respect to other cations.⁶ Concerning dissociative chemisorption, magnesium oxide based materials have received strong attention because of the relatively low temperature of decomposition of the corresponding carbonates.⁷ The capture of CO₂ is only the first step in the carbon dioxide cycle: capture, storage and transportation and underground sequestration. Nevertheless, being the total amount of CO₂ released each year in the atmosphere of the order of gigatons,^{4, 8} finding an effective way to reuse this molecule as valuable chemical reagent as possible alternative to its sequestration,⁹ is a key point in the global warming research. In this perspective, the necessity to identify different CO₂ derivative products is required.¹⁰ Unfortunately, the CO₂ chemical inertia makes this problem even more challenging.

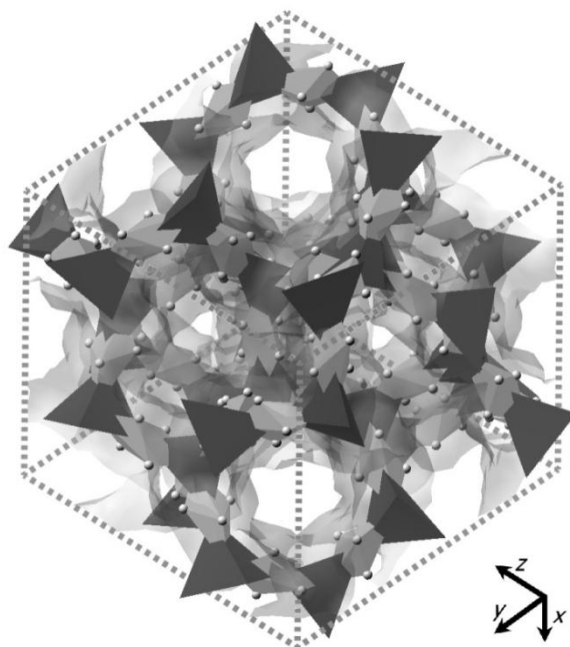


Fig. 1. γ -Mg(BH₄)₂ structure: Mg atoms are represented as dark grey tetrahedra, B atoms as light grey polyhedra and H atoms as spheres. The Connolly surface obtained by using a probe with radius of 1.82 Å is represented.

The open structure of γ -Mg(BH₄)₂ and the large concentration of magnesium cations makes it an ideal material to be studied as CO₂ concentrator. In fact, the proximity to the cation of hydrogen atoms, negatively charged, gives rise to one Lewis basic-acid couple per Mg atom: these couples are well known to be the most suitable ones to enlarge the affinity of unreactive CO₂ toward surfaces.^{11, 12} For example, late transition metal (Ni,Rh) hydrides^{13, 14} instantaneously catalyse the transformation of CO₂ in formate in the presence of borane. Nickel hydride with a diphosphinite-based ligand is an high efficient catalyst for the reduction of CO₂ with

catecholborane, and the hydrolysis of the resulting methoxyboryl species produces CH_3OH in good yield.¹⁵ However, the complex synthesis of these catalysts makes them not applicable to large scale. Methane and ethylene formation for reaction of CO_2 with alanates has been already reported;^{16, 17} nevertheless, this reaction has to be carried out at temperature higher than 120°C in order to observe sufficiently fast kinetics.¹⁷ CO_2 reduction by BH_3NH_3 , LiBH_4 and NaBH_4 was studied previously both theoretically¹⁸ and experimentally,^{19–27} as a method to enhance the thermolytic dehydrogenation of borohydride compounds^{19, 20, 27} or as a cheap method to obtain boron-doped carbons^{21, 22} or graphene oxide.²³ It was also reported that sodium and lithium borohydrides react with CO_2 to give valuable chemical products as formic acid,²⁶ acyloxyborohydrides²⁵ and formatomethoxyborate or triformatoborohydride, depending on reaction conditions (temperature and solvents).²⁴ The separation of the products from the reagents is possible by simply dissolving the material in a suitable solvent (e.g. water,²⁵ although this procedure can be safely adopted only after an high degree of CO_2 conversion has been reached to avoid explosions due to the high exothermicity of unreacted borohydrides reaction with water). Nevertheless, the very low reaction rates at RT (1/90 molar ratio of reacted CO_2/BH_4 after 120 h),²⁴ make unpractical its industrial application.

In this work, the potential of $\gamma\text{-Mg}(\text{BH}_4)_2$ in carbon dioxide recycling are explored for the first time. It is shown as the kinetics of reaction of CO_2 can be enhanced in $\gamma\text{-Mg}(\text{BH}_4)_2$ by several hundreds of time with respect to all previous explored metal hydrides. In order to quantify the CO_2 uptakes, CO_2 isotherms were obtained at 30°C by means of a microbalance, allowing also to investigate the kinetics of the reaction. The effect of the reaction on the structure of $\gamma\text{-Mg}(\text{BH}_4)_2$ were verified by X-Ray powder diffraction (XRPD) and nitrogen adsorption at 77 K whereas the reaction products were identified by means of Fourier Transformed Infrared in attenuated total reflectance spectroscopy (ATR-FTIR) in the medium infrared, coupled with Far-IR investigation and ^{13}C CP-MAS NMR spectroscopy. Moreover, an *in situ* study of the sorption process was performed by FTIR spectroscopy in transmission, in order to get more insights into the reaction mechanism. All the measurements were replicated on the unporous polymorph $\alpha\text{-Mg}(\text{BH}_4)_2$ ($4\text{ m}^2\text{ g}^{-1}$, see Table S1), in order to estimate the importance of the surface/microporosity on the kinetics of the CO_2 conversion.

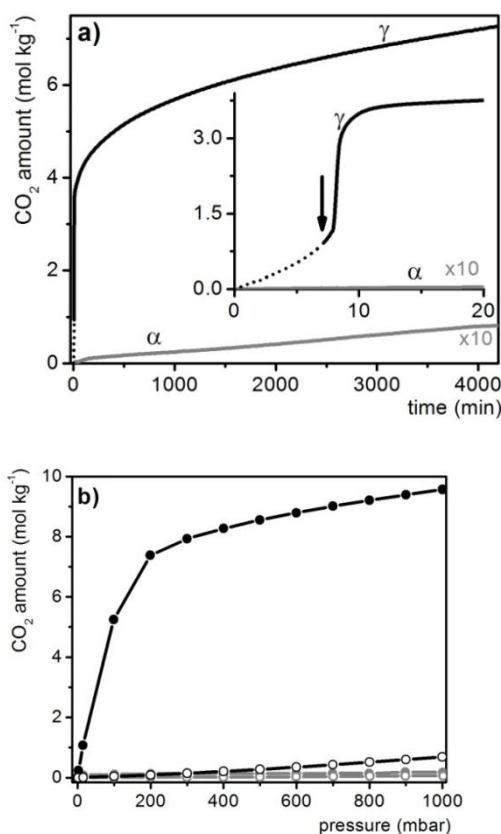


Fig. 2. a) Kinetic curve of CO_2 reaction with $\gamma\text{-Mg}(\text{BH}_4)_2$ at 30°C and 1 bar (black curve). The inset shows the first 20 min of reaction (the arrow indicates the end of the CO_2 dosing procedure). The analogous curve obtained for $\alpha\text{-Mg}(\text{BH}_4)_2$ is reported for comparison (grey curve); the astonishing effect of the increased surface area on the reaction time is well evident. b) CO_2 isotherms on $\gamma\text{-Mg}(\text{BH}_4)_2$ (black curves) and $\alpha\text{-Mg}(\text{BH}_4)_2$ (grey curves) at 30°C (gray curves) obtained by equilibrating the system for 4 h at each pressure. Filled and empty scatters refer to the first and second absorption isotherm, respectively.

The reaction kinetics were evaluated by following the CO_2 uptake as a function of time by means of microgravimetric measurements at 30°C and 1 bar, as shown in Fig. 2a. The $\gamma\text{-Mg}(\text{BH}_4)_2$ phase reaches the impressive value of 1:11 molar ratio of reacted CO_2 for $[\text{BH}_4]^-$ unit after only 10 min. The effect of the surface area on the reaction kinetic is well evident by comparing the data obtained for $\gamma\text{-Mg}(\text{BH}_4)_2$ with those for $\alpha\text{-Mg}(\text{BH}_4)_2$ (black and grey curve, respectively). The absence of highly reactive surface defects on both the $\text{Mg}(\text{BH}_4)_2$ surfaces has been confirmed by an infrared study of CO adsorbed at 100 K (results not shown). Fig. 2b compares the CO_2 isotherms obtained at 30°C for both γ and α phases of $\text{Mg}(\text{BH}_4)_2$. Each point of the isotherms was recorded after a

fixed equilibration time of 4 h; without fixing the time, the equilibration procedure would protract further especially at low pressures. In fact, a plateau value of 12 mol/kg (34.5 mass%) was obtained for the γ phase at 1 bar only after 7 days (data not shown). This value is slightly larger than the highest value reported so far at RT and 1 bar for microporous materials (27.5 mass% in the metal organic frameworks $\text{Mg}_2(\text{dobdc})$ and HKUST-1),²⁸ where CO_2 is molecularly adsorbed in the material pores. Nevertheless, this value is about one half of that reported for the most performing oxidic systems,⁷ although in that case the formation of carbonates and bicarbonates species requires to adopt very high temperatures (e.g. $\text{CaO}/\text{Al}_2\text{O}_3$, 68 mass% at 1 bar and 600°C).⁷ The uptake is completely irreversible, as demonstrated by the second isotherm, indicating that almost the whole material was reacted at the end of the first absorption isotherm. Also in this case, the key-role of the surface area is evident by comparison with the data collected on the α phase.

These results were confirmed by XRPD characterization. Fig. 3 shows the XRPD patterns of $\gamma\text{-Mg}(\text{BH}_4)_2$ before (γ) and after (γ') the reaction with CO_2 . Most of the diffraction peaks present in the pattern of γ disappear in the pattern of γ' , suggesting the complete collapse of the pores structure and the formation of an amorphous phase. The few diffraction peaks still visible are due to a fraction of α phase present as impurity in the starting material (amounting to 16% in volume estimated by Rietveld refinement, see ESI). On the contrary, the crystalline structure of $\alpha\text{-Mg}(\text{BH}_4)_2$ is almost unaffected (α') by the interaction with CO_2 as expected on the basis of the lower CO_2 uptake (see Fig. 2b). In both cases, after the reaction a broad peak is observed at around $2\theta = 13.6^\circ$. It is interesting to notice that a signal in that region, although broader, as well as the formation of an amorphous phase was also observed after thermal dehydrogenation of $\gamma\text{-Mg}(\text{BH}_4)_2$.²⁹ The structure collapse of $\gamma\text{-Mg}(\text{BH}_4)_2$ is confirmed also by nitrogen volumetry, showing a decrease of the surface area of more than two order of magnitude, after reaction with CO_2 (see Table S1 and Electronic Supplementary Information for further details and comments).

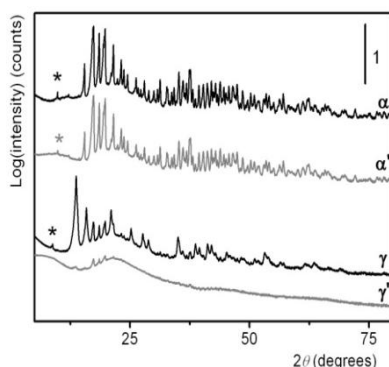


Fig. 3. XRPD patterns of $\gamma\text{-Mg}(\text{BH}_4)_2$ and $\alpha\text{-Mg}(\text{BH}_4)_2$ before (black curves) and after CO_2 interaction at 30°C and 1 bar for 3 days (grey curves).

^{13}C CP-MAS NMR and ATR-IR spectroscopies allowed the identification of the new species formed upon CO_2 sorption. Fig. 4a shows the ATR-IR spectra of the $\gamma\text{-Mg}(\text{BH}_4)_2$ material before and after CO_2 reaction. The IR spectrum of the starting material is quite simple and dominated by the absorption bands related to BH_4 units, at about 2270 cm^{-1} ($\nu(\text{BH}_4)$) and $1258\text{--}1126\text{ cm}^{-1}$ ($\delta(\text{BH}_4)$).²⁹ After prolonged interaction with CO_2 the IR spectrum becomes more complex. The absorption bands characteristic of BH_4 decrease in intensity, although they do not disappear. This observation suggests that the reaction with CO_2 proceeds through a dehydrogenation of $\gamma\text{-Mg}(\text{BH}_4)_2$, but involves only a fraction of the BH moieties (in agreement with the CO_2 sorption measurements). Simultaneously, new IR absorption bands appear, providing an evidence that new chemical species are formed. Although a detailed assignment of all the absorption bands is not straightforward, some of them clearly reveal the formation of formate ($-\text{OOCH}$, band at 1622 cm^{-1} due to $\nu(\text{C=O})$ mode)¹⁹ and methoxy species ($-\text{OCH}_3$, bands in the $3000\text{--}2800\text{ cm}^{-1}$ region due to $\nu(\text{CH}_3)$ and around 1100 cm^{-1} due to $\nu(\text{C-O})$).¹⁹ Finally, the broad absorption band centred around 1300 cm^{-1} are assigned to $\nu(\text{BO})$ mode.^{19, 30} The Far-IR spectra of $\gamma\text{-Mg}(\text{BH}_4)_2$ and $\alpha\text{-Mg}(\text{BH}_4)_2$ phases before (γ and α) and after (γ' and α') the reaction with CO_2 are shown in Fig. 5, compared with that of MgO (taken here as a reference for $\nu(\text{Mg-O})$ vibrations). Both of them are characterized by two sets of absorption bands. The band centered around 425 cm^{-1} (with a shoulder at 377 cm^{-1}) is due to $\nu(\text{Mg-B})$,³¹ whereas the couple of bands centered around 215 cm^{-1} are assigned to $\delta(\text{B-Mg-B})$ vibrational modes.³¹ The two $\delta(\text{B-Mg-B})$ bands have a different intensity ratio in the spectra of the two polymorphs. The Far-IR spectrum of $\alpha\text{-Mg}(\text{BH}_4)_2$ does not change after reaction with CO_2 , in agreement with all the results shown above. On the contrary, the spectrum of γ' is characterized by the almost total disappearance of the absorption bands due to $\delta(\text{B-Mg-B})$ modes; the remaining couple of bands are due to the presence of a small fraction of the α phase, which is unaffected by the reaction with CO_2 , in agreement with XRD data. Moreover, in the spectrum of γ' the $\nu(\text{Mg-B})$ absorption band slightly shifts at lower frequency, accompanied by the appearance of a broad shoulder. All these observations, coupled with the fact that no hydroxyls species (3600 cm^{-1} region) are formed, indicate that most of the reaction products are chemically bounded to B atoms. No evolution of gaseous reaction products (e.g. methane) was evidenced in these temperature and pressure conditions (see Fig. S5).

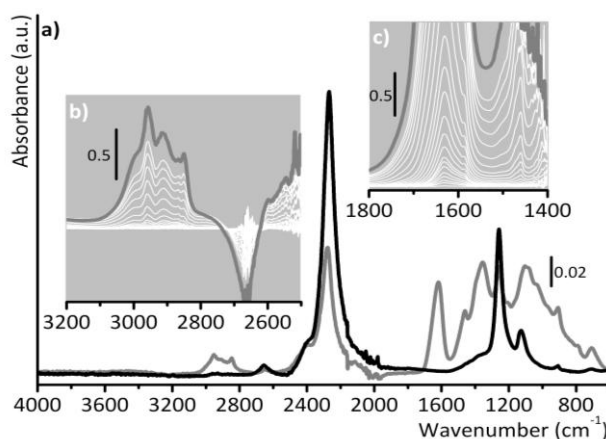


Fig. 4. a): ATR-IR spectra of γ -Mg(BH₄)₂ before (black) and after (dark grey) CO₂ interaction at room temperature and 1 bar for 3 days. b) and c): *in situ* FT-IR spectra collected during reaction of γ -Mg(BH₄)₂ with 100 mbar of CO₂ at room temperature. The last spectrum (dark grey) was collected after 12 hours. The spectra were subtracted from that of the sample before CO₂ dosage.

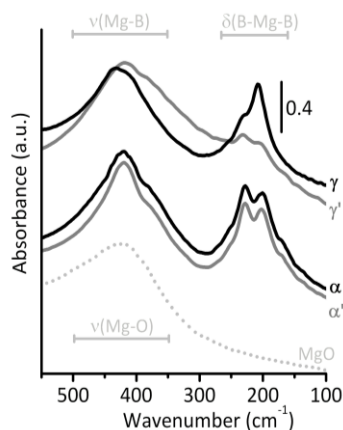


Fig. 5. Far-IR spectra of γ -Mg(BH₄)₂ and α -Mg(BH₄)₂ before (black curves) and after CO₂ interaction at 30°C and 1 bar for 3 days (grey curves). The spectrum of MgO is also shown for comparison.

In order to elucidate the reaction mechanism, the reaction with CO₂ was monitored at room temperature by means of *in situ* FT-IR spectroscopy on samples in the form of self-supporting pellets. Fig. 4b) and c) show the background subtracted sequence of spectra collected at regular time intervals, in the two most relevant wavenumber regions; the spectra in the whole region are reported in the ESI. They demonstrate that formate (band at 1622 cm⁻¹) and methoxy (bands in the 3000-2800 cm⁻¹ region) species are formed simultaneously since the beginning of the reaction at the expenses of BH₄ (bands at 2270 cm⁻¹), and no other reaction intermediates are detected. This is an important difference with respect to what reported for aminoborane reaction with CO₂, where an evolution of the products with time toward compounds with lower valence of carbon is observed.²⁰

Analogous information was obtained by NMR spectroscopy. ¹³C CP MAS spectrum (Fig. 6) is characterized by peaks at 170.7, 85.7, 50.2 and around 33-13 ppm, (33.3, 19.3 and 13.8 ppm), which are characteristics of C=O, OC-H, OCH₃ and aliphatic groups, respectively. This is in agreement with previous results on aminoborane.²⁰ Beside that, NMR allows also to quantify the relative abundance of the reaction products. Interestingly, it is found as the methoxy species (large peak at 50.2 ppm) are the most abundant followed by C=O groups.

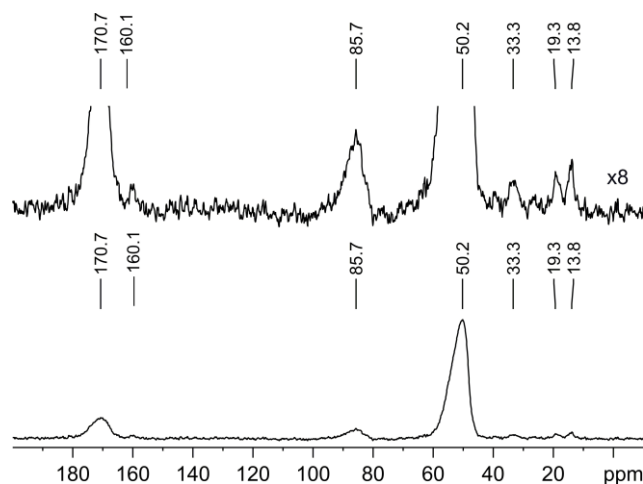


Fig. 6. ^{13}C CPMAS NMR spectrum of $\gamma\text{-Mg}(\text{BH}_4)_2$ sample after CO_2 interaction at RT and 1 bar for 72 h.

In conclusions, the whole set of data discussed above demonstrate that the $\gamma\text{-Mg}(\text{BH}_4)_2$ material efficiently reacts with large amount of CO_2 converting it into valuable chemical products (among which formate and methoxy species). The reaction products can be easily recovered by simple dissolution of the material in water.²⁵ Fast kinetics of reaction were observed, unexpected on the basis of previous results reported for metal hydrides and ascribable to the large surface area of this material. This clearly indicates that this new class of porous metal hydrides are promising materials for CO_2 recycling. The mechanism involves a partial de-hydrogenation of the starting material. The maximum CO_2 uptake, estimated by very prolonged contact time (7 days at 1 bar and 30°C), is about 12 mol/kg. This value is lower than the theoretical one calculated by assuming a 1:1 reaction between CO_2 and BH_4 (37.0 mol/kg, corresponding to 62 mass%), but it is very close to that expected by considering the completeness of the first step in the dehydrogenation of $\gamma\text{-Mg}(\text{BH}_4)_2$ (12.3 mol/kg, corresponding to 35 mass%).³² This first step is characterized by an almost complete reversibility.^{33, 34} In this respect, the results shown herein acquire interesting perspectives: if re-hydrogenable, $\gamma\text{-Mg}(\text{BH}_4)_2$ could be used as catalyst for CO_2 transformation into valuable organic products instead as reagent. Preliminary attempts in this direction were at the moment unsuccessful for both performing the reaction in a CO_2/H_2 atmosphere or by exposing the sample to 20 bar of H_2 at 250°C after the reaction, likely because of the higher CO_2 interaction energy with respect to H_2 and the large stability of the B-O bond. Nevertheless, the very fast kinetics associated to the reaction would provide to this hydride the peculiar characteristics to be able to couple in one step the separation (in post combustion systems) and recycling of CO_2 in a wide temperature range ($\text{RT} < T < 190^\circ\text{C}$) allowing to avoid the storage and transportation steps. The possibility to use $\gamma\text{-Mg}(\text{BH}_4)_2$ as co-reagents in other CO_2 -based reactions would enlarge the number of obtainable products and will be the subject of future investigations.

Acknowledgements

Financial support by PRIN (2010-2011) is acknowledged. Dr. M. R. Chierotti is strongly acknowledged for the ^{13}C NMR measurements.

Notes and references

^a Department of Chemistry, NIS Center and INSTM reference Center, Università di Torino, via Quarellotto 15, I-10135 Torino, Italy.

^b (present address) Department of Science and High Technology, Università dell'Insubria, Via Lucini 3, 22100 Como, Italy, Tel.: +39 031-2386614; Fax: +39 031-2386630; E-mail: jenny.vitillo@uninsubria.it.

^c Institute of Nanotechnology, Karlsruhe Institute of Technology (KIT), Hermann-von-Helmholtz-Platz 1, 76344 Eggenstein-Leopoldshafen, Germany.

† Electronic Supplementary Information (ESI) available: samples and experimental methods details, *in situ* FTIR in transmission of CO_2 reaction with $\text{Mg}(\text{BH}_4)_2$ samples, Nitrogen adsorption measurements and Rietveld refinements results of the materials before and after reaction with CO_2 , IR spectrum of the gas phase composition after CO_2 reaction with $\gamma\text{-Mg}(\text{BH}_4)_2$ for 3 days. See DOI: 10.1039/b000000x/

- Y. Filinchuk, B. Richter, T. R. Jensen, V. Dmitriev, D. Chernyshov and H. Hagemann, *Angew. Chem. Int. Ed.*, 2011, **50**, 11162–11166.
- J. R. Petit, J. Jouzel, D. Raynaud, N. I. Barkov, J. M. Barnola, I. Basile, M. Bender, J. Chappellaz, M. Davis, G. Delaygue, M. Delmotte, V. M. Kotlyakov, M. Legrand, V. Y. Lipenkov, C. Lorius, L. Pepin, C. Ritz, E. Saltzman and M. Stievenard, *Nature*, 1999, **399**, 429–436.
- <http://www.esrl.noaa.gov/gmd/ccgg/trends/>, 2014.
- M. Mikkelsen, M. Jorgensen and F. C. Krebs, *Energy Environ. Sci.*, 2010, **3**, 43–81.
- J. P. Laboratory, <http://sealevel.jpl.nasa.gov/>.
- S. R. Caskey, A. G. Wong-Foy and A. J. Matzger, *J. Am. Chem. Soc.*, 2008, **130**, 10870–10871.
- S. Wang, S. Yan, X. Ma and J. Gong, *Energy Environ. Sci.*, 2011, **4**, 3805–3819.
- E. A. Quadrelli, G. Centi, J. L. Duplan and S. Perathoner, *Chem. Sus. Chem.*, 2011, **4**, 1194–1215.
- D. S. Goldberg, T. Takahashi and A. L. Slagle, *Proc. Natl. Acad. Sci. U. S. A.*, 2008, **105**, 9920–9925.
- D. M. D'Alessandro, B. Smit and J. R. Long, *Angew. Chem.-Int. Edit.*, 2010, **49**, 6058–6082.
- R. Vaidhyanathan, S. S. Iremonger, G. K. H. Shimizu, P. G. Boyd, S. Alavi and T. K. Woo, *Science*, 2010, **330**, 650–653.

12. J. G. Vitillo, M. Savonnet, G. Ricchiardi and S. Bordiga, *Chem. Sus. Chem.*, 2011, **4**, 1281-1290.
13. S. R. Miller, P. A. Wright, T. Devic, C. Serre, G. Ferey, P. L. Llewellyn, R. Denoyel, L. Gaberova and Y. Filinchuk, *Langmuir*, 2009, **25**, 3618-3626.
14. Y. Jiang, O. Blacque, T. Fox and H. Berke, *J. Am. Chem. Soc.*, 2013, **135**, 7751-7760.
15. S. Chakraborty, J. Zhang, J. A. Krause and H. Guan, *J. Am. Chem. Soc.*, 2010, **132**, 8872-8873.
16. B. T. Thompson, T. N. Gallaher and T. C. DeVore, *Polyhedron*, 1983, **2**, 619-621.
17. C. L. Hugelshofer, A. Borgschulte, E. Callini, S. K. Matam, J. Gehrig, D. T. Hog and A. Züttel, *J. Phys. Chem. C*, 2014, **118**, 15940-15945.
18. P. M. Zimmerman, Z. Zhang and C. B. Musgrave, *Inorg. Chem.*, 2010, **49**, 8724-8728.
19. J. Zhang, Y. Zhao, D. L. Akins and J. W. Lee, *J. Phys. Chem. C*, 2011, **115**, 8386-8392.
20. R. Xiong, J. S. Zhang and J. W. Lee, *J. Phys. Chem. C*, 2013, **117**, 3799-3803.
21. J. S. Zhang and J. W. Lee, *Carbon*, 2013, **53**, 216-221.
22. J. S. Zhang, A. Byeon and J. W. Lee, *J. Mater. Chem. A*, 2013, **1**, 8665-8671.
23. J. S. Zhang, Y. Zhao, X. D. Guan, R. E. Stark, D. L. Akins and J. W. Lee, *J. Phys. Chem. C*, 2012, **116**, 2639-2644.
24. T. Wartik and R. K. Pearson, *J. Inorg. Nuclear Chem.*, 1958, **7**, 404-411.
25. G. W. Gribble and C. F. Nutaitis, *Org. Prep. Proced. Int.*, 1985, **17**, 317-384.
26. J. G. Burr, W. G. Brown and H. E. Heller, *J. Am. Chem. Soc.*, 1950, **72**, 2560-2562.
27. R. Xiong, J. Zhang, Y. Zhao, D. L. Akins and J. W. Lee, *Int. J. Hydrogen En.*, 2012, **37**, 3344-3349.
28. K. Sumida, D. L. Rogow, J. A. Mason, T. M. McDonald, E. D. Bloch, Z. R. Herm, T. H. Bae and J. R. Long, *Chem. Rev.*, 2012, **112**, 724-781.
29. M. Paskevicius, M. P. Pitt, C. J. Webb, D. A. Sheppard, U. Filsø, E. MacA. Gray and C. E. Buckley, *J. Phys. Chem. C*, 2012, **116**, 15231-15240.
30. E. Culea and I. Bratu, *Acta Mater.*, 2001, **49**, 123-125.
31. J. W. Nibler, *J. Am. Chem. Soc.*, 1972, **94**, 3349-3359.
32. W. I. F. David, S. K. Callear, M. O. Jones, P. C. Aeberhard, S. D. Culligan, A. H. Pohl, S. R. Johnson, K. R. Ryan, J. E. Parker, P. P. Edwards, C. J. Nuttall and A. Amieiro-Fonseca, *Phys. Chem. Chem. Phys.*, 2012, **14**, 11800-11807.
33. M. Chong, A. Karkamkar, T. Autrey, S.-i. Orimo, S. Jalisatgid and C. M. Jensen, *Chem. Commun.*, 2011, **47**, 1330-1332.
34. C. M. Jensen and M. Chong, *FY 2012 Annual Progress Report*, 2012.